

Article

# Assessing Land Degradation Dynamics and Distinguishing Human-Induced Changes from Climate Factors in the Three-North Shelter Forest Region of China

Senwang Huang <sup>1,2</sup> and Jiming Kong <sup>1,\*</sup>

<sup>1</sup> Key Laboratory of Mountain Hazards and Earth Surface Processes, Institute of Mountain Hazards and Environment, Chinese Academy of Sciences, Sichuan 610041, China; huangsenwang@163.com

<sup>2</sup> University of Chinese Academy of Science, Beijing 100049, China

\* Correspondence: jimingk@imde.ac.cn; Tel.: +86-136-5807-1828

Academic Editors: Yichun Xie, Xinyue Ye and Wolfgang Kainz

Received: 15 May 2016; Accepted: 19 August 2016; Published: 2 September 2016

**Abstract:** Land degradation is a major threat to the sustainability of human habitation, and it is essential to assess it quantitatively. Assessment of the human-induced aspect is especially important for planning appropriate prevention measures. This paper used the Three-North Shelter Forest Program region as the study area, and assessed the land degradation dynamic using a time series of summed normalized difference vegetation index (NDVI) based on a trend analysis of the Theil-Sen slope and Mann-Kendall test. The human-induced land degradation was separated from degradation driven by climate using the meteorological dataset through the residual trend (RESTREND) method for the period 1982–2006. The results showed that (1) the NDVI in the study area mainly exhibited an increasing trend, approximately 13.00% of the study area experienced significantly positive NDVI trends and 6.20% showed decline. Furthermore, (2) the correlation between the summed NDVI and precipitation was higher than the correlation between NDVI and temperature, suggesting that precipitation was the most essential factor that impacted NDVI dynamic in the study area; (3) The significant trends of vegetation by anthropogenic disturbances were detected, which were significant positive and negative trends of 11.93% and 6.19%, respectively. All of these findings enrich our knowledge of human activities that impact land degradation in arid or semi-arid regions and provide a scientific basis for the management of ecological restoration programs.

**Keywords:** land degradation; Three-North Shelter Forest Program (TNSFP); NDVI; trend analysis; human factors

## 1. Introduction

Land degradation is one of the most serious global environmental issues of this time period. It can be defined as the persistent/long-term reduction of ecosystem services and vegetation productivity of the land, and it affects the lives of large numbers of people [1–4]. This phenomenon includes diverse processes, involving changes in plant species composition, soil erosion, and the reduction of the land's productive potential [2,5]. The dynamics of degradation can be caused by both human factors and natural processes [2,6]. Human causes include the overuse of land (e.g., overgrazing and deforestation) and other socio-economic factors, such as improper agriculture development policies [7,8]. Natural factors include extreme and periodic climatic variations; aridity and droughts, mainly induced by precipitation and temperature in arid or semi-arid regions [9–11].

On a national or global scale, one of the obstacles is a lack of robust data and methodologies to monitor and assess land degradation [12]. From the definition of land degradation, the land dynamics

mainly impact of the above-ground vegetation production and, therefore, vegetation production has been generally used as a measurement of land degradation on a national or global scale [13]. Earth observation is most frequently employed to monitor the above-ground vegetation processes with the availability of satellite time-series data covering the past three decades and nearly all the world [10]. Thus, to some extent, remote sensing is a crucial tool to map land degradation, and vegetation production may be the single most useful indicator of land degradation from time-series satellite images at regional or global scales [11,14,15]. Many researchers have taken net primary production (NPP) as an indicator to evaluate vegetation production trends to assess land degradation [16–18]. Nevertheless, the estimates of NPP are not only complicated but also limited [19]. NPP could not be directly monitored by Earth observation (EO) methods and was usually estimated based on the Carnegie-Ames-Stanford Approach (CASA) model [20,21]. Several parameters of the model (e.g., climate, vegetation type and soil type) are all estimated indirectly and may contain spatial heterogeneity and uncertainty. Moreover, in arid or semi-arid areas the Normalized Difference Vegetation Index (NDVI) is strongly correlated with above-ground net primary productivity (ANPP) [22–24]. As a result, one of the most widely used approaches is based on the seasonal sums of NDVI, which may be summed over the growing seasons to obtain the multi-temporal  $\Sigma$ NDVI, which is assumed to be a proxy for ANPP in arid or semi-arid areas [10].

Distinguishing different types of factors that affect vegetation degradation is a central environmental and socioeconomic issue in dryland research and is essential for recognizing and managing vegetation productivity changes [2,25,26]. The relationship between climate factors and NDVI have been accustomed to separate causes of productivity changes, and any NDVI variations not explained by climatic dynamics are attributed to human activities [4,27,28]. However, there is a challenge on how to distinguish vegetation productivity variations due to climatic factors from those caused by human activities on large spatial and long temporal scales. Rain-use efficiency (RUE) has been suggested as an index for evaluating land degradation by means of normalizing the precipitation variability, and many researchers have attempted to utilize this ratio to measure non-precipitation related land degradation [15,18]. Nevertheless, RUE ratios are still largely related to precipitation, since trends of RUE only manifest the variations of rainfall [26]. Residual Trend (RESTREND) analysis [29] has been manifested to be a more robust approach than the RUE ratio [7,30].

China is one country affected by land degradation, especially in the Three-North regions (the northeast, north, northwest). The Three-North Shelter Forest Program (TNSFP) is the largest afforestation reconstruction project in the world, with approximately 2/3 of the area arid or semi-arid, and aims to control sand storms and soil erosion through increasing forest coverage. There is a continuing argument against the strength of the Chinese national ecological engineering projects [31]. On one hand, many researchers in China found that the ecological effects of ecological restoration programs are positive as a whole and have combated desertification and dust storms successfully [32–35]. On the other hand, a few experts thought that afforestation programs may not perform well in semi-arid and arid regions, and there was not enough evidence to support statements that the large-scale ecological restoration program might have some positive effects on reducing desertification and dust storms [31]. Consequently, it is very important to estimate land degradation dynamics and distinguish the human dimension. Previous research indicates that NDVI-based approaches for evaluating land degradation ought to be continually validated in different geographical areas [36]. Thus far, in China, trend analysis has not been conditioned for estimating the vegetation production dynamics and the predisposing factors of land degradation have not been detected in a systematical unequivocal way on such a long-term and national scale. Suitability and validity of RESTREND, particularly when applied in different arid or semi-arid regions, would still need to be estimated. Therefore, the objectives of this study were to (1) assess the land degradation dynamic using the growing season  $\Sigma$ NDVI; (2) analyze the relationships between  $\Sigma$ NDVI and meteorological data (precipitation and temperature); and (3) distinguish human-induced land degradation from climate driven impacts.

## 2. Materials and Methods

### 2.1. Study Area

The Chinese government has begun the TNSFP to plant shelter forests throughout the Northern China for combating severe environmental degradation from 1979. The TNSFP region involves 551 counties located in 13 provinces in north China, ranging from  $73^{\circ}26'E$  to  $127^{\circ}50'E$  and from  $33^{\circ}30'N$  to  $50^{\circ}12'N$  (Figure 1). It covers most of the Northern China, with a distance of 4480 km from Bin County of Heilongjiang Province in the east to the Wuzhibeli Mountain pass in the west and a range from 560 to 1440 km from south to north. The total area is 4.069 million  $km^2$ , accounting for approximately 42.4% of the land area of China [9].

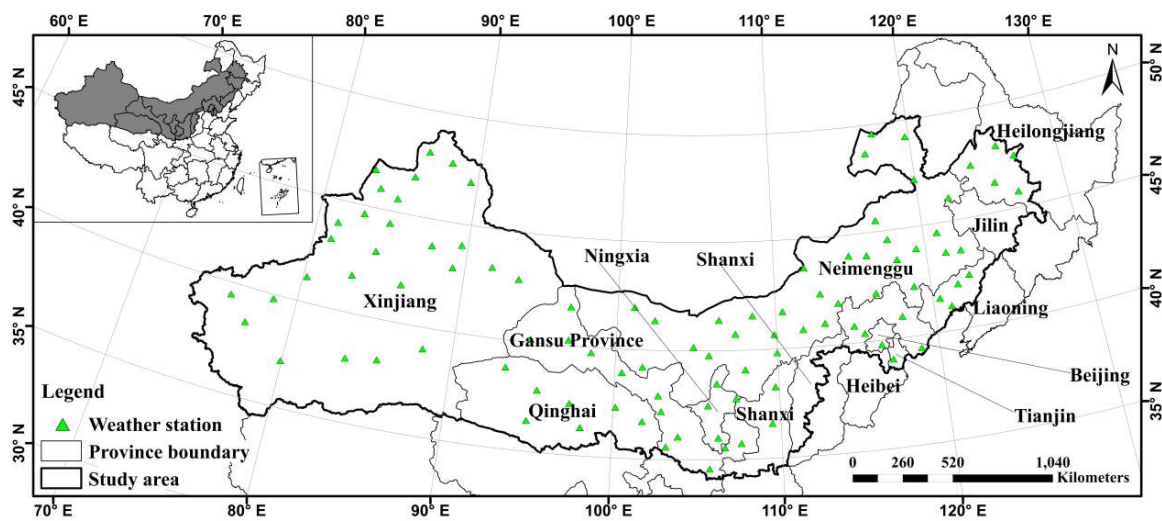


Figure 1. Location map of the study area in China.

The study area includes arid, semi-arid, and semi-arid semi-humid climates, with precipitation decreases moving from east to west and from south to north, ranging from less than 50 mm to more than 400 mm. The temperature differences across the region, along with the annual average temperature decreases from  $-9.7^{\circ}C$  in the northeast to  $14^{\circ}C$  in the south, and with the average temperature in most areas ranging from  $2-8^{\circ}C$ . The elevation increases from east to west, includes plains, plateaus, and mountains [37]. The droughts and floods occur frequently, because the ecological environment is fragile, the time of sunshine is longer, the rainfall is less and human activities are more concentrated in the TNSFP region [38].

### 2.2. NDVI Dataset

The NDVI products used in this study were the Global Inventory Modelling and Mapping Studies (GIMSS) NDVI datasets from 1982-2006. The NDVI products were obtained from GIMSS group based on NOAA/AVHRR estimates with 8-km spatial resolution and a 15-day temporal resolution. The geometric, radiation, and atmospheric corrections were performed according to the methods of [39,40], and then for every day and every track image, bad lines and clouds were removed. Furthermore, the maximum-value composite (MVC) method was used to eliminate the influence of clouds, the atmosphere, and the solar elevation angle. To reflect the vegetation cover more appropriately, the NDVI products were summed over the entire growing season and minimum and maximum values were removed [26].

### 2.3. Metrological Data

Rainfall and temperature data were collected by a network of approximately 120 weather stations provided by National Meteorological Information Center of China. Data were averaged for every 10-day period of the year at each station. The growth-season-summed rainfall (April–October) was used here as the measurement since it had a strong relationship with growth season summed NDVI [7,41]. The gridded rainfall and temperature surfaces of the study area were then created using multiple linear regression models with independent variable layers (altitude, latitude, longitude) for every weather station. The deviations (standard errors of the estimate) of the regression equation were interpolated over the total area using inverse distance weighting. The predicted climate data were calculated by altitude, latitude, and longitude based on DEM data (1 km). The results of climate data were equal to the summation of deviation layers and predicted values. The climate data were resampled to match the GIMMS data using a bilinear resampling algorithm.

### 2.4. Trend Analysis

Temporal trends of the  $\Sigma$ NDVI were analyzed using a Theil-Sen (Sen) slope, which is a robust non-parametric statistical estimation of the trend magnitude and is especially insensitive to small outliers and missing noises values [42,43]. Statistical significance of the Sen slope trend was tested using the Mann-Kendall (MK) significance test, which is widely applied to long-time series trend analysis with non-normal data [7,41,44]. The threshold of z scores using for testing the significance was 1.96 at 95% confidence level ( $\alpha = 0.05$ ) over time, which provided both the significance and direction of the trend. The algorithm was implemented by Interface Description Language.

### 2.5. The Correlation Method

Correlations between NDVI and climate factors (rainfall and temperature) were calculated using the least square regression method on a per-pixel basis for the period of 1982–2006 [45]. The statistical significance was tested using Pearson's correlation coefficients at a confidence level of 90% ( $\alpha = 0.1$ ). Since vegetation production might not continue to increase linearly with rainfall, the rainfall values were changed by logarithm transformation [44,46]. If the correlation coefficient was greater than 0.3 (F-test,  $\alpha = 0.1$ , the degrees of freedom: 23), it was considered that inter-annual NDVI had a strong correlation with climate factors. The significance of Pearson's correlation coefficient was mapped to show geographical distribution of the relationships.

### 2.6. The RESTREND Method

If the significant climate effects could be removed from the long-term trends of NDVI, human-induced land degradation might be distinguished [25,29]. The RESTREND method was widely used in removing factors from the vegetation trends, especially at large scales, and was based on the general condition that vegetation production was positively correlated with impact factors (rainfall and temperature) in arid or semiarid ecosystems [2]. Regressions between growth season summed NDVI and  $\log_e$  Rainfall were calculated for each pixel in the above-mentioned area. The statistical model was then used to generate the predicted values of the cumulative NDVI at each pixel. The residuals were the differences between the observed and predicted NDVI values and were analyzed to detect the trend over time. If there was a significant decreasing trend of residuals, it would presumably be derived by human activities. Otherwise, if the residuals showed no trend over time, the declining vegetation production would be attributed to climate factors such as rainfall and temperature.

### 3. Results

#### 3.1. The Accumulated NDVI Dynamic

The Sen slope value was calculated for the growing season accumulated NDVI products using the trend analysis method for the periods 1982–2006 (Figure 2). The vegetation production trend was positive overall, shown by the average NDVI change in each year (Figure 3). Nevertheless, the mean NDVI ( $R = 0.22$ ,  $P = 0.50$ ) showed no significantly increasing trends. Figure 2 illustrates that most of the positive trends were in the northwest and northeast regions of the study area. The positive trends in the northwest were mainly in the Tianshan Mountains and the oasis areas of the Tarim River; and the positive trends in the northeast were located in the province of Heilongjiang, Jilin, and Hebei. However, small areas in these regions had negative trends, mainly in the Liaoning province and the loess plateau.

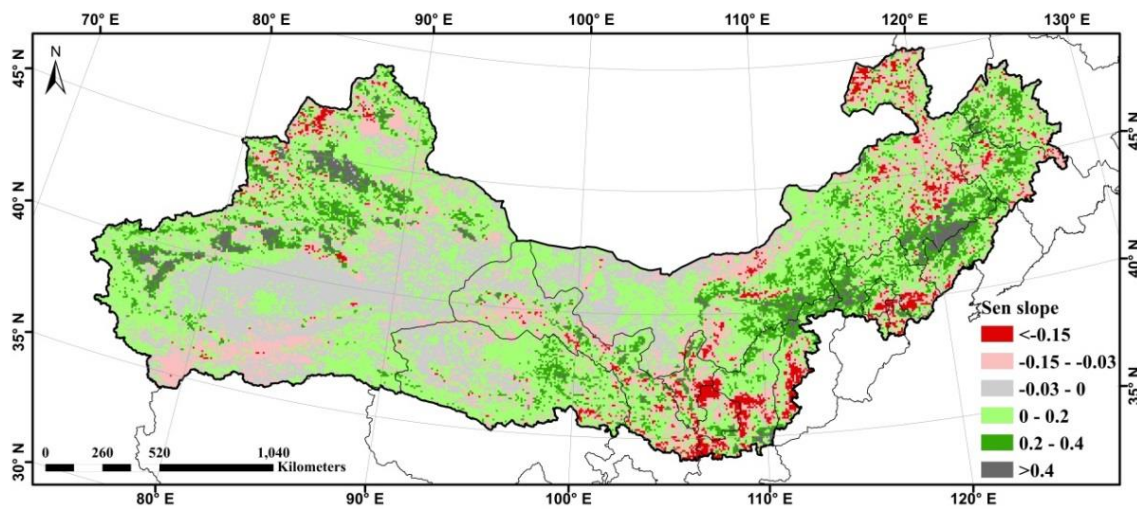


Figure 2. Spatial pattern of the Sen slope of the NDVI time-series in growth seasons from 1982–2006.

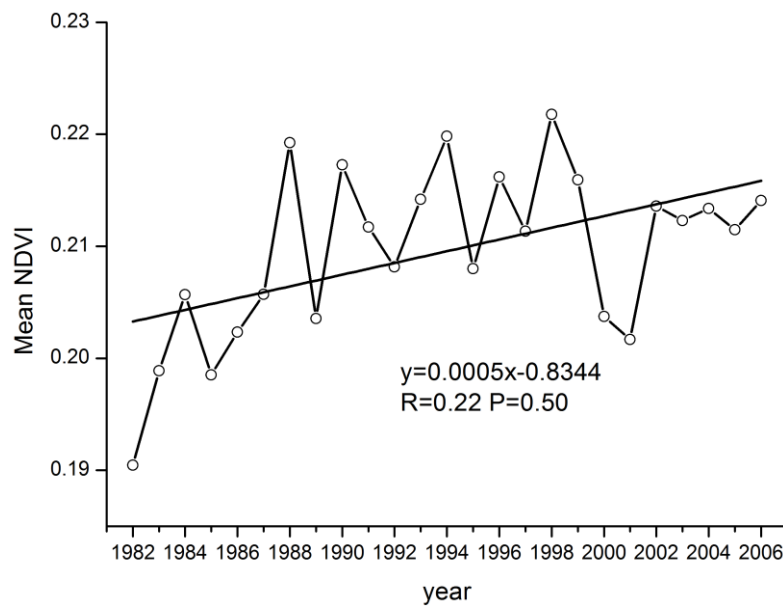


Figure 3. Inter-annual variations of the average NDVI in growth season from 1982–2006 in the TNSFP region.

To remove the non-vegetative impact, the settlement and cropland land-use types were masked by land use of 2005. The significant trends of vegetation were tested by the MK test over the last 25 years, with the results showing that 13.00% of the TNSFP significantly increased and 6.20% decreased significantly at 95% confidence level (Figure 4).

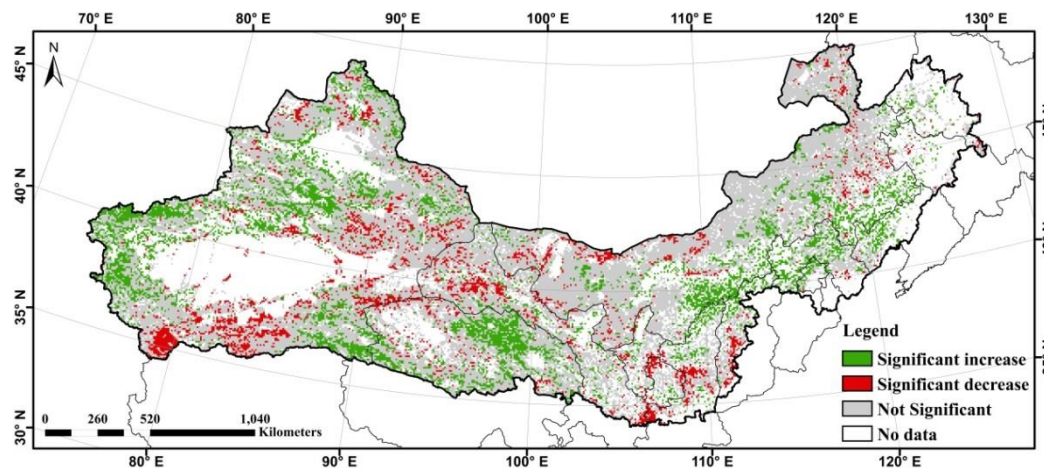


Figure 4. Spatial pattern of significant change for the accumulated NDVI in growth seasons from 1982–2006.

### 3.2. The Relationships between NDVI and Climate Data

#### 3.2.1. The Relationships between NDVI and Precipitation

Figure 5 showed the geographical distribution of the significant correlation between summed NDVI and precipitation at a 90% confidence level for the time period of 1982–2006. The statistical analysis revealed that 41.34% of the pixels were positively correlated 14.42% of which were significantly positively correlated and primarily located in the north of the Xinjiang Province and most of Inner Mongolia Province (Figure 5, Table 1).

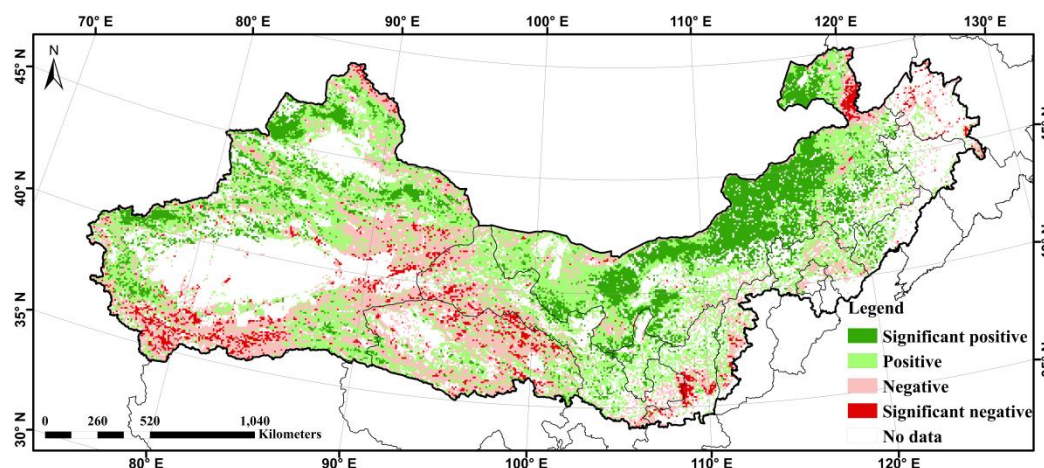


Figure 5. Significant correlation of the accumulated NDVI with  $\log_e$  Rainfall for the growing seasons.

Table 1. Statistics of significant correlation between the accumulated NDVI and rainfall.

Correlation	Significant Positive	Positive	Negative	Significant Negative	Stable
Pixel numbers (8 km)	8862	16,542	13,049	2249	20,738
Proportion statistics (%)	14.42	26.92	21.24	3.66	33.76

### 3.2.2. The Relationships between NDVI and Temperature

The spatial distribution of the significant correlation between summed NDVI and annual mean temperature was mapped at a confidence level of 90% for the period of 1982–2006 (Figure 6). The distribution showed that NDVI was not significantly correlated with mean temperature for most pixels. The proportion statistical analysis showed that only 2.42% of pixels were significantly positively correlated, and the significant negative correlation was 1.88% (Table 2).

Results from this study and previous research [9] indicate that the correlation between NDVI and precipitation was stronger than that between NDVI and temperature. Numerous researchers [2,9,46–48] have stated a lack of water in arid or semi-arid regions, resulting in precipitation being the major climate factor of vegetation production. It was concluded that precipitation was the most important climate factor of vegetation production in the TNSFP region.

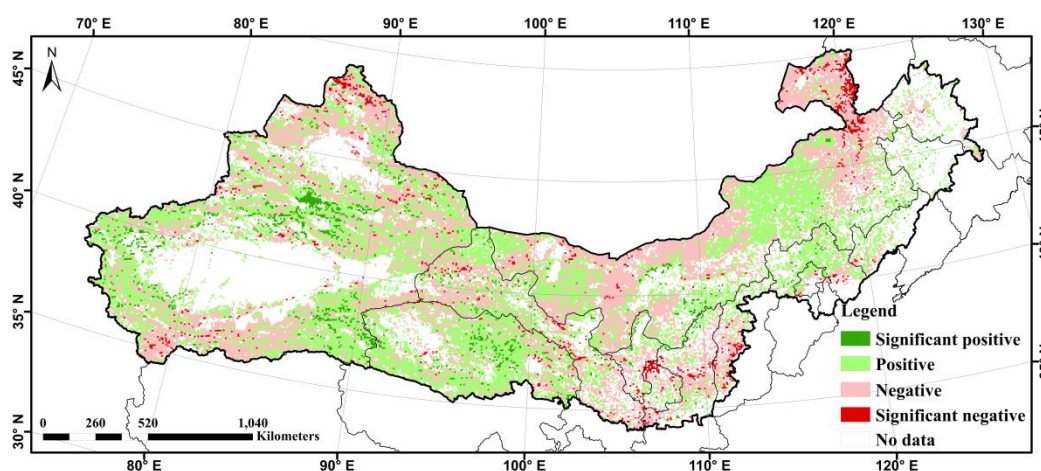


**Figure 6.** Significant correlation between the accumulated NDVI and annual mean temperature from 1982–2006.

**Table 2.** Statistics of significant correlation between the accumulated NDVI and annual mean temperature.

Correlation	Significant Positive	Positive	Negative	Significant Negative	Stable
Pixel numbers (8 km)	1484	18,871	18,891	1153	20,868
Proportion statistics (%)	2.42	30.80	30.83	1.88	34.06

### 3.3. Land Degradation induced by Human Factors

Since the RESTREND method was based on the assumption that there was a strong relationship between vegetation production and climate factors, rainfall was used to simulate the natural impact on vegetation production [30]. Since not all areas were significantly correlated in terms of  $\Sigma$ NDVI-rainfall, a combined RESTREND- $\Sigma$ NDVI slope approach was used to distinguish human-induced vegetation productivity. Firstly, where rainfall had a dominant positive impact on vegetation production, the human-induced vegetation productivity was detected by the RESTREND method. Secondly, the significance of  $\Sigma$ NDVI slope was induced by human activities, where rainfall had a dominant negative impact on vegetation production. Thirdly, where  $\Sigma$ NDVI-rainfall did not show a statistically significant trend, the significant changes of  $\Sigma$ NDVI slope were largely induced by human factors. Finally, the human-induced land degradation was obtained through overlay analysis of the above results in Geographic Information System (GIS) (Figure 7).

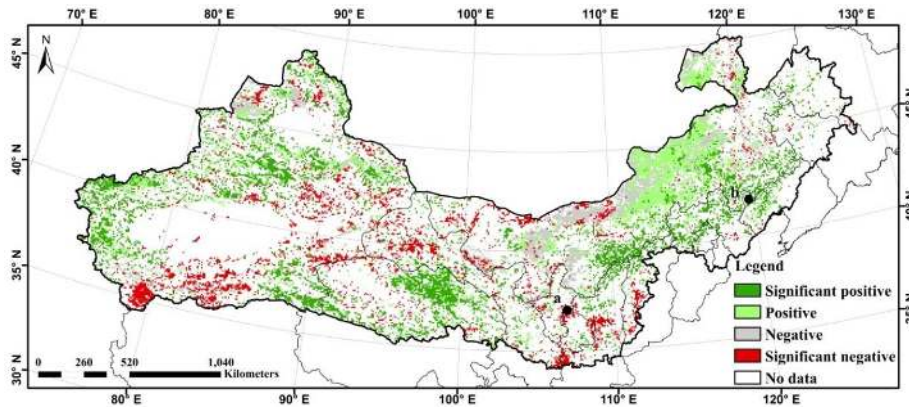


**Figure 7.** Spatial pattern of the significant changes in vegetation production induced by human activities.

The regeneration regions were mainly in the northern portion of Xinjiang Province, the northeastern portion of the Qinghai Province, and along a northeast-to-southwest bank along the boundary of the Inner Mongolia Province. The degradation areas were largely in the Loess Plateau and a northeast-to-southwest bank in Xinjiang Province. Moreover, we summarized the percentage of the significant vegetation production changes that increased/decreased by human factors (Table 3). The percentage of changes in significantly increased areas was 11.93%, and in significantly decreased areas, it was 11.93%.

**Table 3.** Statistics of significant effects for human-induced vegetation change.

Mann-Kendall Test	Significant Positive	Positive	Negative	Significant Negative	Stable
Pixel numbers (8 km)	7328	4565	4342	3803	41,402
Proportion statistics (%)	11.93	7.43	7.07	6.19	67.38

To detect the effects of removing rainfall variability on vegetation production for individual years, a profile analysis of two samples (a, b in Figure 7) was carried out between residuals and rainfall based on 3×3 pixels (Figure 8). Sample a was located in the Huan country of Gansu Province, where land degradation was serious because of overgrazing. Sample b was located in the southern portion of the Horqin Sandy Land, where vegetation increased evidently due to a program that converted cropland to forest.

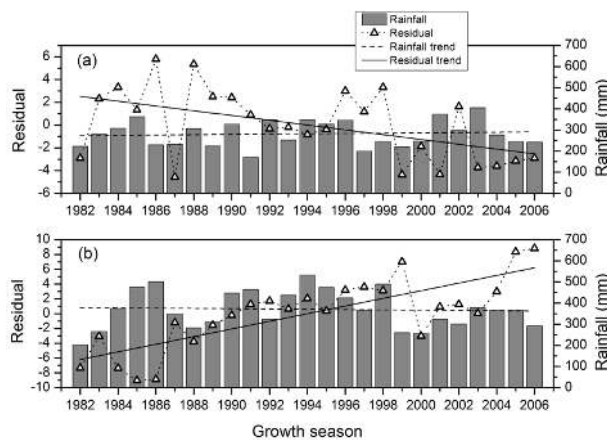


**Figure 8.** Trend of residuals plotted against rainfall per growth seasons for the typical samples: (a) The location of significant decrease for residuals; (b) The location of significant increase for residuals.



Since country-wide vegetation monitoring programs are rare, it was very difficult to validate if regions indicating negative residual trends were indeed being degraded at the national scale over such a long time period [18]. Higher spatial resolution of Landsat data was used to verify the trends qualitatively by using the false color composite (FCC). Due to the different image acquisition time, radiometric calibration was performed based on MODTRAN 4 (MODerate spectral resolution atmospheric Transmittance algorithm and computer model version 4). The time of each image was selected close to the beginning and end of the time series. Figure 9 shows regeneration with positive changes in northeast of Qinghai Province, and Figure 10 shows land degradation with negative changes in the middle of Inner Mongolia Province.

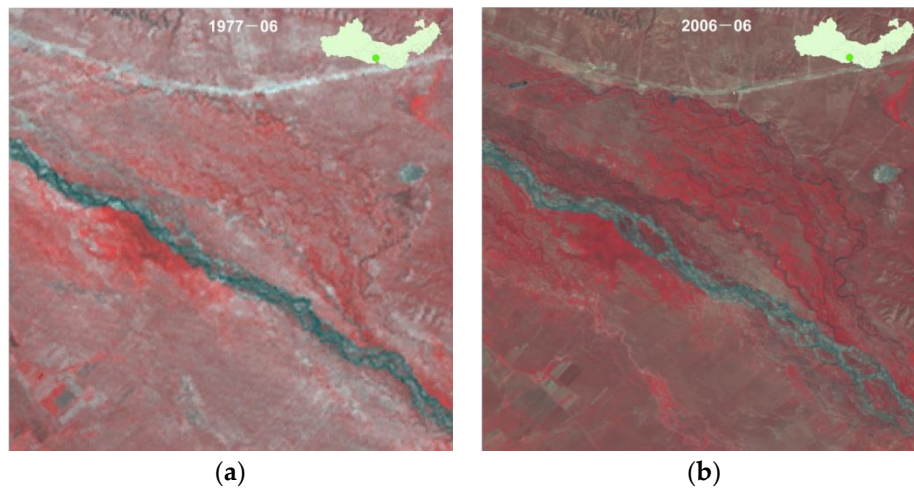


**Figure 9.** The significant positive changes of vegetation production by human activities in northeast of Qinghai Province: (a) MSS image in June 1977; and (b) TM image in June 2006.

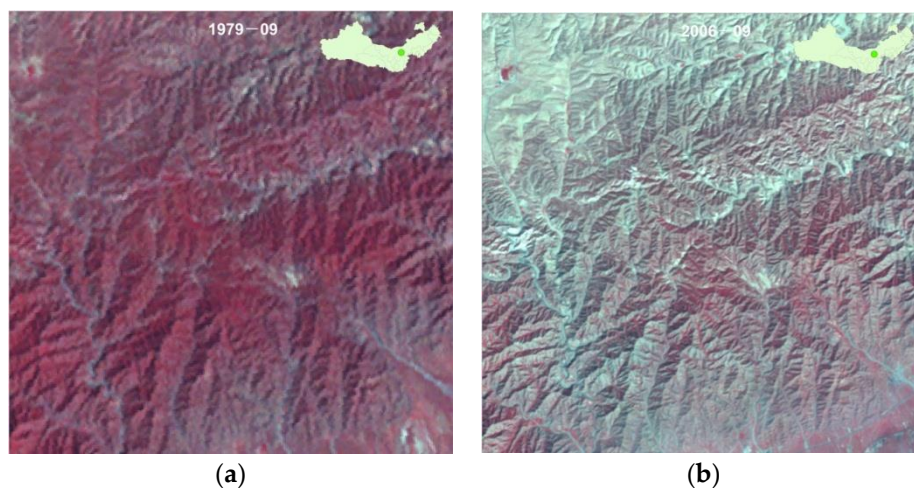


**Figure 10.** The significant negative changes of vegetation production by human activities in the middle of Inner Mongolia Province: (a) MSS image in September 1977; and (b) TM image in September 2006.

## 4. Discussion

### 4.1. Trends of Vegetation Activity in the TNSFP Region

Vegetation production in most areas of the TNSFP region showed an overall increase over the past 25 years, suggesting that the ecological restoration program was effective. The vegetation distribution and change trend result were consistent with the previous literature that used direct

field measurements [49] or ANPP. This result indicates that the use of  $\Sigma$ NDVI as a proxy of ANPP is a feasible method for assessment of the vegetation pattern in the ecosystem [9,50]. The result of the non-parametric MK trends test in this study was very similar to other results by linear regression [9]. Nevertheless, it is advisable to use the non-parametric methods in trend analysis since they not only meet all assumptions, but are also more robust in terms of the satellite time-series data.

#### 4.2. Impacts of Climate Factors on the Vegetation Production

In general, variations in vegetation production had permanently been linked with changes in climate at a variety of spatial and temporal scales as a result of climatic and anthropogenic causes [51,52]. In the study area, most of the pixels showed a significant positive correlation between NDVI and precipitation, but the relationship between NDVI and temperature was weak. The finding was consistent with many previous studies that showed that vegetation production in arid or semi-arid regions was very sensitive to rainfall changes [27,53]. The rising temperature had dual influences, when water was sufficiently available, rising temperature improved photosynthetic efficiency and increased vegetation productivity. On the other hand, the warming increased evapotranspiration and even led to drought, particularly in arid or semi-arid regions, thereby decreasing photosynthetic rates. Furthermore, Northern China was affected by severe droughts in 2000 and 2001 [54,55]. As a result, precipitation was the major climate factor in vegetation productivity, particularly in arid or semi-arid regions.

#### 4.3. Impacts of Human Activities on the Vegetation Production

The residual trend analysis result indicated that human activities had a greater positive effect on vegetation change. TNSFP divided the program's periods from 1978 to 2010 into four periods (1978–1985, 1986–1995, 1996–2000, and 2001–2010). Figure 1a shows that the positive residual had an obvious regularity with time periods. The ecological restoration programme was the major human activity at this scale, with programs, such as grassland managements; conversion of cropland to grassland or forest; and afforestation and reforestation by closing hill or aerial seeding. Furthermore, the negative effects of irrational anthropogenic activities, such as overgrazing and reclamation, could offset the positive impacts of ecological restoration program on vegetation production in these areas (Figure 1b).

The significant relationship between vegetation production and rainfall was the basic premise of the RESTREND method. Severe human disturbances could change the vegetation types and localized redistributions of water, which might weaken this relationship [56]. If there was degradation, the relationship would also generally decouple the predicted vegetation production in the RESTREND method, which would undervalue the magnitude of degradation [30].

#### 4.4. Limitations

The spatial and temporal scales of the time series could impact the results of the residual trend analysis. The coarse spatial resolution of the remote sensing dataset (GIMMS) used in the study was confined by the availability of data on temporal scales. Since coarse resolution data might neglect some vital details, using finer-scaled data could improve the accuracy of the analysis and provide better detectable power and results [57]. Degradation results were underestimated near the beginning or end of the time-series since negative trends in residuals would be very difficult to detect when occurring in the first or last two years of the time-series [58,59].

The validation of trend analysis is another very important issue and a major concern, which requires a comparable spatial and temporal field biomass dataset. However, it was rarely possible to obtain direct field measurements at these large scales. The simulation approach proposed by Wessels et al. [30] might provide the direction for the development of a consistent and wide-range validation methodology.

Due to the lack of relevant observation data, our approach did not determine the reference value of land degradation quantitatively or analyze the types of human factors. Thus, there are still some challenges for future studies on the quantitative estimation and cause of land degradation in the TNSFP.

## 5. Conclusions

This paper explored the variation in trend of vegetation production based a long-term series of inter-annual AVHRR NDVI in the TNSFP region of China. By analyzing the relationships between climate factors (rainfall and temperature) and NDVI time series over the last 25 years, we distinguished the areas of productivity change impacted by human activities from those affected by climate dynamics.

The main conclusions found in the study are summarized as follows:

1. The vegetation production of the TNSFP region showed an overall positive trend from 1982 to 2006: with a significant proportion of 13.00% and 47% with stable trends.
2. There were considerably more significant positive correlations between NDVI and precipitation than those between NDVI and temperature. Therefore, precipitation had a great impact on vegetation growth, with 41.34% of the pixels positively correlated with precipitation, with 14.42% significance at the 95% significance level.
3. The results suggested that the RESTREND method combined with trend analysis was a useful tool for controlling the effects of rainfall in order to detect human-induced land degradation. An apparent increasing trend was shown in 11.93% of pixels, and only 6.19% of pixels showed statistically significant degradation, implying that the ecological restoration program was effective in the TNSFP region.

**Acknowledgments:** This study was supported by the Foundation of National 863 Plan of China (No. 2012AA121302), Key Deployment Research Program of CAS (No. KZZD-EW-05-01-02) and the National Key Basic Research Program of China (No. 2015CB452704 and 2013CB733205). We are grateful to the anonymous reviewers for their valuable comments and recommendations.

**Author Contributions:** Senwang Huang and Jiming Kong conceived and designed the experiments; Senwang Huang analyzed the data and wrote the paper.

**Conflicts of Interest:** The authors declare no conflict of interest.

## Abbreviations

The following abbreviations are used in this manuscript:

ANPP	above-ground net primary productivity
DEM	Digital Elevation Model
EO	Earth observation
FCC	false color composite
GIS	Geographic Information System
GIMSS	the Global Inventory Modeling and Mapping Studies
MK	Mann-Kendall
MVC	the maximum-value composite
NDVI	normalized difference vegetation index
NPP	net primary production
RESTREND	the residual trend
RUE	Rain-Use Efficiency
Sen	Theil-Sen
TNSFP	Three-North Shelter Forest Program

## References

1. Reynolds, J.F.; Stafford Smith, D.M.; Lambin, E.F.; Turner, B.L.; Mortimore, M.; Batterbury, S.P.J.; Downing, T.E.; Dowlatabadi, H.; Fernandez, R.J.; Herrick, J.E.; et al. Global desertification: Building a science for dryland development. *Science* **2007**, *316*, 847–851. [[CrossRef](#)] [[PubMed](#)]

2. Wessels, K.J.; Prince, S.D.; Malherbe, J.; Small, J.; Frost, P.E.; Van Zyl, D. Can human-induced land degradation be distinguished from the effects of rainfall variability? A case study in south africa. *J. Arid Environ.* **2007**, *68*, 271–297. [[CrossRef](#)]
3. Bai, Z.G.; Dent, D.L.; Olsson, L.; Schaepman, M.E. Proxy global assessment of land degradation. *Soil Use Manag.* **2008**, *24*, 223–234. [[CrossRef](#)]
4. Le, Q.B.; Tamene, L.; Vlek, P.L.G. Multi-pronged assessment of land degradation in West Africa to assess the importance of atmospheric fertilization in masking the processes involved. *Glob. Planet. Chang.* **2012**, *92–93*, 71–81. [[CrossRef](#)]
5. Pickup, G. Estimating the effects of land degradation and rainfall variation on productivity in rangelands: An approach using remote sensing and models of grazing and herbage dynamics. *J. Appl. Ecol.* **1996**, *33*, 819–832. [[CrossRef](#)]
6. Eckert, S.; Hüsler, F.; Liniger, H.; Hodel, E. Trend analysis of MODIS NDVI time series for detecting land degradation and regeneration in Mongolia. *J. Arid Environ.* **2015**, *113*, 16–28. [[CrossRef](#)]
7. Prince, S.D.; De Colstoun, E.B.; Kravitz, L.L. Evidence from rain-use efficiencies does not indicate extensive sahelian desertification. *Glob. Chang. Biol.* **1998**, *4*, 359–374. [[CrossRef](#)]
8. Duan, H.C.; Yan, C.Z.; Tsunekawa, A.; Song, X.; Li, S.; Xie, J.L. Assessing vegetation dynamics in the three-north shelter forest region of China using AVHRR NDVI data. *Environ. Earth Sci.* **2011**, *64*, 1011–1020. [[CrossRef](#)]
9. Vu, Q.M.; Le, Q.B.; Vlek, P.L.G. Hotspots of human-induced biomass productivity decline and their social-ecological types toward supporting national policy and local studies on combating land degradation. *Glob. Planet. Chang.* **2014**, *121*, 64–77. [[CrossRef](#)]
10. Mbow, C.; Brandt, M.; Ouedraogo, I.; de Leeuw, J.; Marshall, M. What four decades of earth observation tell us about land degradation in the Sahel? *Remote Sens.* **2015**, *7*, 4048–4067. [[CrossRef](#)]
11. Veron, S.R.; Paruelo, J.M.; Oesterheld, M. Assessing desertification. *J. Arid Environ.* **2006**, *66*, 751–763. [[CrossRef](#)]
12. De Jong, R.; de Bruin, S.; Schaepman, M.; Dent, D. Quantitative mapping of global land degradation using earth observations. *Int. J. Remote Sens.* **2011**, *32*, 6823–6853. [[CrossRef](#)]
13. Pickup, G.; Bastin, G.N.; Chewings, V.H. Remote-sensing-based condition assessment for nonequilibrium rangelands under large-scale commercial grazing. *Ecol. Appl.* **1994**, *4*, 497–517. [[CrossRef](#)]
14. Fensholt, R.; Rasmussen, K.; Kaspersen, P.; Huber, S.; Horion, S.; Swinnen, E. Assessing land degradation/recovery in the African Sahel from long-term earth observation based primary productivity and precipitation relationships. *Remote Sens.* **2013**, *5*, 664–686. [[CrossRef](#)]
15. Holm, A.M.; Cridland, S.W.; Roderick, M.L. The use of time-integrated NOAA NDVI data and rainfall to assess landscape degradation in the arid shrubland of Western Australia. *Remote Sens. Environ.* **2003**, *85*, 145–158. [[CrossRef](#)]
16. Liu, S.L.; Wang, T. Aeolian desertification from the mid-1970s to 2005 in Otindag sandy land, northern China. *Environ. Geol.* **2007**, *51*, 1057–1064. [[CrossRef](#)]
17. Prince, S.D.; Becker-Reshef, I.; Rishmawi, K. Detection and mapping of long-term land degradation using local net production scaling: Application to Zimbabwe. *Remote Sens. Environ.* **2009**, *113*, 1046–1057. [[CrossRef](#)]
18. Fensholt, R.; Rasmussen, K. Analysis of trends in the sahelian ‘rain-use efficiency’ using gimms NDVI, RFE and GPCP rainfall data. *Remote Sens. Environ.* **2011**, *115*, 438–451. [[CrossRef](#)]
19. Potter, C.S.; Randerson, J.T.; Field, C.B.; Matson, P.A.; Vitousek, P.M.; Mooney, H.A.; Klooster, S.A. Terrestrial ecosystem production—A process model-based on global satellite and surface data. *Glob. Biogeochem. Cycles* **1993**, *7*, 811–841. [[CrossRef](#)]
20. Yuan, J.G.; Niu, Z.; Wang, C.L. Vegetation NPP distribution based on MODIS data and CASA model—A case study of northern Hebei province. *Chin. Geogr. Sci.* **2006**, *16*, 334–341. [[CrossRef](#)]
21. Pettorelli, N.; Vik, J.O.; Mysterud, A.; Gaillard, J.M.; Tucker, C.J.; Stenseth, N.C. Using the satellite-derived NDVI to assess ecological responses to environmental change. *Trends Ecol. Evol.* **2005**, *20*, 503–510. [[CrossRef](#)] [[PubMed](#)]
22. Wessels, K.J.; Prince, S.D.; Zambatis, N.; Macfadyen, S.; Frost, P.E.; Van Zyl, D. Relationship between herbaceous biomass and 1-km(2) advanced very high resolution radiometer (AVHRR) NDVI in Kruger national park, south Africa. *Int. J. Remote Sens.* **2006**, *27*, 951–973. [[CrossRef](#)]

23. Fensholt, R.; Langanke, T.; Rasmussen, K.; Reenberg, A.; Prince, S.D.; Tucker, C.; Scholes, R.J.; Le, Q.B.; Bondeau, A.; Eastman, R.; et al. Greenness in semi-arid areas across the globe 1981–2007—An earth observing satellite based analysis of trends and drivers. *Remote Sens. Environ.* **2012**, *121*, 144–158. [[CrossRef](#)]
24. Archer, E.R.M. Beyond the “climate versus grazing” impasse: Using remote sensing to investigate the effects of grazing system choice on vegetation cover in the eastern Karoo. *J. Arid Environ.* **2004**, *57*, 381–408. [[CrossRef](#)]
25. Wessels, K.J. Comments on ‘proxy global assessment of land degradation’ by bai et al. (2008). *Soil Use Manag.* **2009**, *25*, 91–92. [[CrossRef](#)]
26. Herrmann, S.M.; Anyamba, A.; Tucker, C.J. Recent trends in vegetation dynamics in the African Sahel and their relationship to climate. *Glob. Environ. Chang* **2005**, *15*, 394–404. [[CrossRef](#)]
27. Li, S.H.; Xiao, J.T.; Xu, W.B.; Yan, H.M. Modelling gross primary production in the Heihe river basin and uncertainty analysis. *Int. J. Remote Sens.* **2012**, *33*, 836–847. [[CrossRef](#)]
28. Evans, J.; Geerken, R. Discrimination between climate and human-induced dryland degradation. *J. Arid Environ.* **2004**, *57*, 535–554. [[CrossRef](#)]
29. Wessels, K.J.; van den Bergh, F.; Scholes, R.J. Limits to detectability of land degradation by trend analysis of vegetation index data. *Remote Sens. Environ.* **2012**, *125*, 10–22. [[CrossRef](#)]
30. Wang, X.M.; Zhang, C.X.; Hasi, E.; Dong, Z.B. Has the three norths forest shelterbelt program solved the desertification and dust storm problems in arid and semiarid China? *J. Arid Environ.* **2010**, *74*, 13–22. [[CrossRef](#)]
31. Wang, G.Y.; Innes, J.L.; Lei, J.F.; Dai, S.Y.; Wu, S.W. Ecology—China’s forestry reforms. *Science* **2007**, *318*, 1556–1557. [[CrossRef](#)] [[PubMed](#)]
32. Liu, J.G.; Li, S.X.; Ouyang, Z.Y.; Tam, C.; Chen, X.D. Ecological and socioeconomic effects of China’s policies for ecosystem services. *Proc. Natl. Acad. Sci. USA* **2008**, *105*, 9477–9482. [[CrossRef](#)] [[PubMed](#)]
33. Yang, X.H.; Ci, L.J. Comment on “why large-scale afforestation efforts in china have failed to solve the desertification problem”. *Environ. Sci. Technol.* **2008**, *42*, 7722–7723. [[CrossRef](#)] [[PubMed](#)]
34. Yin, R.S.; Yin, G.P. China’s primary programs of terrestrial ecosystem restoration: Initiation, implementation, and challenges. *Environ. Manag.* **2010**, *45*, 429–441. [[CrossRef](#)] [[PubMed](#)]
35. Vogt, J.V.; Safriel, U.; Von Maltitz, G.; Sokona, Y.; Zougmore, R.; Bastin, G.; Hill, J. Monitoring and assessment of land degradation and desertification: Towards new conceptual and integrated approaches. *Land Degrad Dev.* **2011**, *22*, 150–165. [[CrossRef](#)]
36. Liu, L.Y.; Tang, H.; Caccetta, P.; Lehmann, E.A.; Hu, Y.; Wu, X.L. Mapping afforestation and deforestation from 1974 to 2012 using Landsat time-series stacks in Yulin District, a key region of the three-north shelter region, China. *Environ. Monit. Assess.* **2013**, *185*, 9949–9965. [[CrossRef](#)] [[PubMed](#)]
37. Chong, D.L.S.; Mougou, E.; Gastelluetchegorry, J.P. Relating the global vegetation index to net primary productivity and actual evapotranspiration over Africa. *Int. J. Remote Sens.* **1993**, *14*, 1517–1546. [[CrossRef](#)]
38. Tucker, C.J.; Pinzon, J.E.; Brown, M.E.; Slayback, D.A.; Pak, E.W.; Mahoney, R.; Vermote, E.F.; El Saleous, N. An extended avhrr 8-km NDVI dataset compatible with MODIS and SPOT vegetation NDVI data. *Int. J. Remote Sens.* **2005**, *26*, 4485–4498. [[CrossRef](#)]
39. Piao, S.; Yin, G.; Tan, J.; Cheng, L.; Huang, M.; Li, Y.; Liu, R.; Mao, J.; Myneni, R.B.; Peng, S.; et al. Detection and attribution of vegetation greening trend in China over the last 30 years. *Glob. Chang. Biol.* **2015**, *21*, 1601–1609. [[CrossRef](#)] [[PubMed](#)]
40. Yang, X.; Liu, S.; Yang, T.; Xu, X.; Kang, C.; Tang, J.; Wei, H.; Ghebregabher, M.G.; Li, Z. Spatial-temporal dynamics of desert vegetation and its responses to climatic variations over the last three decades: A case study of Hexi region in northwest China. *J. Arid Land* **2016**, *8*, 556–568. [[CrossRef](#)]
41. Wang, J.; Price, K.P.; Rich, P.M. Spatial patterns of NDVI in response to precipitation and temperature in the central great plains. *Int. J. Remote Sens.* **2001**, *22*, 3827–3844. [[CrossRef](#)]
42. Theil, H. A rank-invariant method of linear and polynomial regression analysis. In *Econometric Theory and Methodology*; Springer: Amsterdam, The Netherlands, 1950; pp. 386–392.
43. Sen, P.K. Estimates of the regression coefficient based on Kendall’s Tau. *J. Am. Stat. Assoc.* **1968**, *63*, 1379–1389. [[CrossRef](#)]
44. Milich, L.; Weiss, E. GAC NDVI images: Relationship to rainfall and potential evaporation in the grazing lands of the gourma (northern Sahel) and in the croplands of the Niger-nigeria border (southern Sahel). *Int. J. Remote Sens.* **2000**, *21*, 261–280. [[CrossRef](#)]

45. Rutherford, M.C. Annual plant-production precipitation relations in arid and semi-arid regions. *S. Afr. J. Sci.* **1980**, *76*, 53–56.
46. Rosenzwe, M.L. Net primary productivity of terrestrial communities—Prediction from climatological data. *Am. Nat.* **1968**, *102*, 67–74. [[CrossRef](#)]
47. Lehouerou, H.N.; Bingham, R.L.; Skerbek, W. Relationship between the variability of primary production and the variability of annual precipitation in world arid lands. *J. Arid Environ.* **1988**, *15*, 1–18.
48. Ji, L.; Peters, A.J. A spatial regression procedure for evaluating the relationship between AVHRR-NDVI and climate in the northern great plains. *Int. J. Remote Sens.* **2004**, *25*, 297–311. [[CrossRef](#)]
49. Fang, J.; Chen, A.; Peng, C.; Zhao, S.; Ci, L. Changes in forest biomass carbon storage in China between 1949 and 1998. *Science* **2001**, *292*, 2320–2322. [[CrossRef](#)] [[PubMed](#)]
50. Wu, Z.T.; Wu, J.J.; Liu, J.H.; He, B.; Lei, T.J.; Wang, Q.F. Increasing terrestrial vegetation activity of ecological restoration program in the Beijing-Tianjin sand source region of China. *Ecol. Eng.* **2013**, *52*, 37–50. [[CrossRef](#)]
51. Justice, C.O.; Hiernaux, P.H.Y. Monitoring the grasslands of the sahel using NOAA AVHRR data-niger 1983. *Int. J. Remote Sens.* **1986**, *7*, 1475–1497. [[CrossRef](#)]
52. Piao, S.L.; Fang, J.Y.; Zhou, L.M.; Guo, Q.H.; Henderson, M.; Ji, W.; Li, Y.; Tao, S. Interannual variations of monthly and seasonal normalized difference vegetation index (NDVI) in China from 1982 to 1999. *J. Geophys. Res. Atmos.* **2003**, *108*, 1–13. [[CrossRef](#)]
53. Chen, G.S.; Tian, H.Q.; Zhang, C.; Liu, M.L.; Ren, W.; Zhu, W.Q.; Chappelka, A.H.; Prior, S.A.; Lockaby, G.B. Drought in the southern united states over the 20th Century: Variability and its impacts on terrestrial ecosystem productivity and carbon storage. *Clim. Chang.* **2012**, *114*, 379–397. [[CrossRef](#)]
54. Piao, S.L.; Ciais, P.; Huang, Y.; Shen, Z.H.; Peng, S.S.; Li, J.S.; Zhou, L.P.; Liu, H.Y.; Ma, Y.C.; Ding, Y.H.; et al. The impacts of climate change on water resources and agriculture in China. *Nature* **2010**, *467*, 43–51. [[CrossRef](#)] [[PubMed](#)]
55. Barriopedro, D.; Gouveia, C.M.; Trigo, R.M.; Wang, L. The 2009/10 drought in China: Possible causes and impacts on vegetation. *J. Hydrometeorol.* **2012**, *13*, 1251–1267. [[CrossRef](#)]
56. Buyantuyev, A.; Wu, J. Urbanization alters spatiotemporal patterns of ecosystem primary production: A case study of the phoenix metropolitan region, USA. *J. Arid Environ.* **2009**, *73*, 512–520. [[CrossRef](#)]
57. Higginbottom, T.P.; Symeonakis, E. Assessing land degradation and desertification using vegetation index data: Current frameworks and future directions. *Remote Sens.* **2014**, *6*, 9552–9575. [[CrossRef](#)]
58. Prince, S.D.; Wessels, K.J.; Tucker, C.J.; Nicholson, S.E. Desertification in the Sahel: A reinterpretation of a reinterpretation. *Glob. Chang. Biol.* **2007**, *13*, 1308–1313. [[CrossRef](#)]
59. Hein, L.; de Ridder, N.; Hiernaux, P.; Leemans, R.; de Wit, A.; Schaepman, M. Desertification in the Sahel: Towards better accounting for ecosystem dynamics in the interpretation of remote sensing images. *J. Arid Environ.* **2011**, *75*, 1164–1172. [[CrossRef](#)]

